Computational Electrochemistry: The Boundary Element Method

Q. Fulian and A. C. Fisher*

Department of Chemistry, University of Bath, Claverton Down, Bath BA2 7AY, U.K.

Received: April 28, 1998

The boundary element (BE) method is presented as an efficient and powerful method for the analysis of electrochemical processes. The paper describes the theory and numerical details required to develop steady state, one-, two-, and three-dimensional diffusional models for voltammetric simulations. The reduction in dimensionality brought about by the application of BE method for processes is noted, along with the resulting benefits when applied to electrochemical systems. The versatility and efficiency of the numerical procedures are examined with respect to a number of electrode geometries. In the case of 2D procedures the simulation of a microdisk and microhemispherical geometries are evaluated and the results compared to the analytical behavior. The change in current density observed as the hemispherical electrode is sequentially flattened to a microdisk is then described. Three-dimensional simulations focus on modeling a microdisk electrode which is then distorted. The resulting current density obtained for a range of three-dimensional gemoetries are noted. The potential of the BE method for examing irregular electrode geometries is also noted.

Introduction

The rapid development of electrochemical techniques over the past decade has resulted in a wide variety of novel analytical techniques and devices.[1−5] Along with this expansion has come the requirement for accurate and efficient numerical models which essentially allow the quantification of the data obtained. For the majority of workers this numerical modeling has been performed using finite difference (FD) techniques of various forms.[6−10] These FD techniques offer a relatively straightforward introduction to the simulation of electrolysis reactions. However the FD approaches have some significant limitations which have led workers in the related engineering and materials fields to look for alternative strategies.[11−13] In particular the FD formulation makes the simulation of irregular geometries difficult due to the point approximation employed. Two of the most popular alternatives amoungst the engineering community have been the finite element (FE) and boundary element (BE) methods. Although considerably different in formulation these two methods allow the mapping of unusual or irregular shapes relatively easily, without resorting to enormous numbers of mesh points.

We have recently presented applications of the FE method in hydrodynamic and diffusional mass transport regimes, which were shown to offer benefits over the FD approach in the field of electrochemistry. In this paper we explore the application of the BE method to electrochemical processes under diffusion control. This particular method has yet to be exploited fully by the electrochemical field yet has enormous advantages in term of numerical speed and flexibility. Previous electrochemical applications of the BE method have focused on predominately on engineering aspects;[14−20] in this article we explore the potential geometries of considerably smaller dimensions and focus on the primary current distribution around electrodes of experimental interest.

The BE method begins with the weighted residual formulation of the appropriate mass transport equation followed by its integration twice to produce the inverse formulation.[21,22] By careful selection of the weigthing function it is possible to obtain an integral representation which results in the order of the differential being reduced. This integral is then discretised over the boundary and solved by standard numerical matrix routines. This is perhaps the most significant benefit of the BE approach since it gives rise to a reduction in the dimensionality of the problem. For example consider the solution of the 2-dimensional form of the Laplace equation

$$k_x\left(\frac{\partial^2\phi}{\partial x^2}\right) + k_y\left(\frac{\partial^2\phi}{\partial y^2}\right) = 0 \qquad (1)$$

The grid discretization to solve this problem for an arbitary geometry using FD, FE, and BE techniques is shown in Figure 1. Both the FD and FE approaches require a grid over the whole domain; however, the BE method only requires elements around the boundary. The benefits of the dimensionality reduction are 2-fold: first the simulation time is substantially reduced in comparison to the other approaches and second the grid generation is a far simpler, a not insignificant problem in the simulation of complex geometries.

Further benefits from the electrochemical viewpoint arise since the BE method produces the flux at the boundaries directly and consequently the requirement for large numbers of grid points close to the electrode surface apparent in FD and FE methods to accurately caluclate the flux are not required.

In this paper we begin our exploration of the BE method for voltammetric studies. Specifically we present the general formulation and numerical procedures for solving one-, two- and three-dimensional diffusion dominated problems under steady-state mass transport conditions. In this article we focus on establishing the accuracy and efficiency of the BE technique by simulating the behavior of well defined and analytically calculable geometries. One-dimensional simulations focus of the flux of material down a line. The two-dimensional solutions first explore microdisk and hemispherical electrodes. Following these calculations the current density of intermediate geometries between these two geometries are calculated. This problem is difficult to tackle analytically yet requires only the smallest of modifications to the gird positions using the BE approach.

10.1021/jp982030i CCC: $15.00
Published on Web 11/26/1998

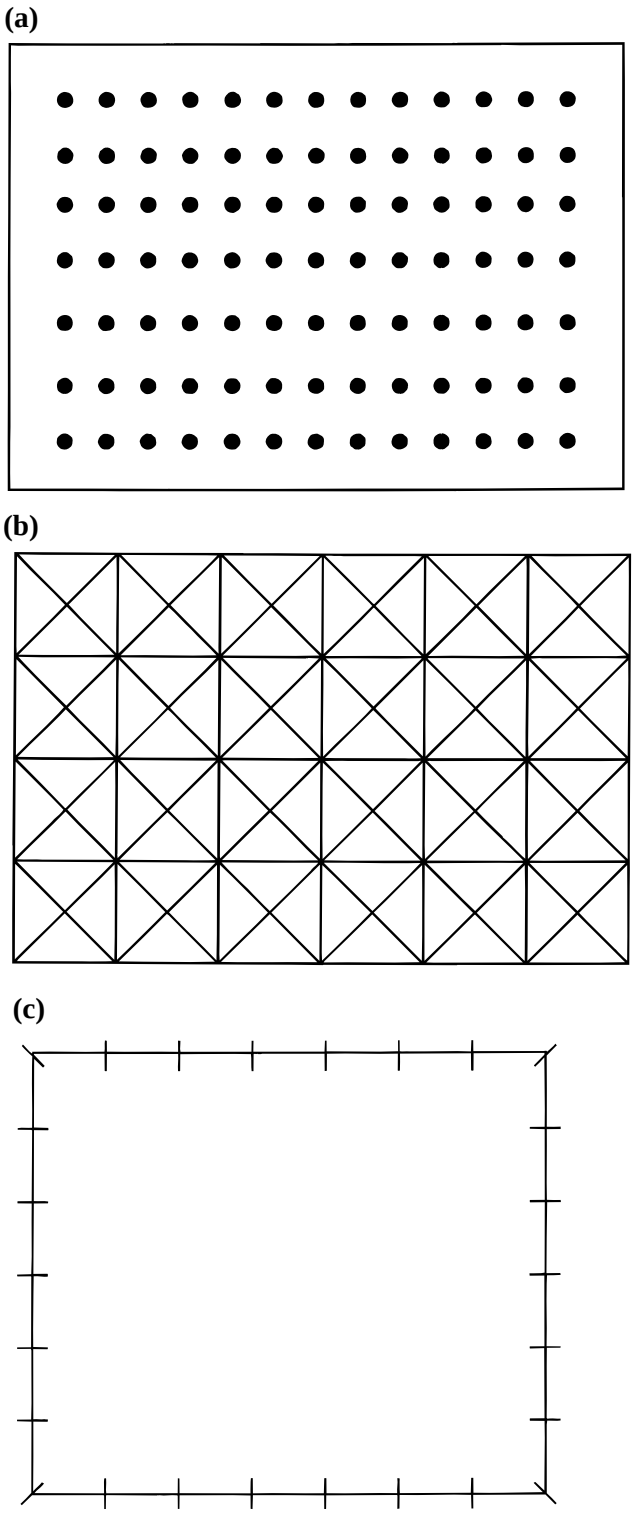

Figure 1. Schematic of the computational grids required for (a) finite difference, (b) finite element, and (c) boundary element solution of the two-dimensional Laplace equation.

Finally, three-dimensional simulations are performed to assess the change in current density as a microdisk is distorted in a three-dimensional manner.

Theory

For the purposes of this paper we shall consider the transport limited one electron reduction

$$A(s) + e^{-}(m) \rightarrow B(s)$$

Under transport conditions where diffusion is dominate, solution of the Laplace eq 2 along with the appropriate boundary conditions enables the prediction of the electrolysis current for a voltammetric measurement.

$$\nabla^2 c = 0 \tag{2}$$

Migratory effects may be ignored when sufficient electrolyte is added to the electrolysis solution and consequently are not addressed within the article. Depending upon the dimensionality of the problem the Laplace equation can be simplified to

$$D_A\left(\frac{\partial^2 c}{\partial x^2}\right) + D_A\left(\frac{\partial^2 c}{\partial y^2}\right) + D_A\left(\frac{\partial^2 c}{\partial z^2}\right) = 0 \tag{3}$$

for typical electrochemical measurements, where D is the diffusion coefficient of the species (A) and x, y, and z represent the Cartesian coordinates. Formulation of the integrals follow the same basic path whether the one-, two-, or three-dimensional form of the Laplace equation is required. For clarity we will therefore present the basic approach for one-dimensional problems and then note the appropriate procedure alterations for two and three-dimensional cases.

Consider the Laplace equation in one dimension

$$\frac{\partial^2 c}{\partial x^2} = 0 \tag{4}$$

where the dimension x now represents a ratio of the distance divided by the diffusion coefficient. This can be represented in operator notation as

$$\mathbf{L}c = 0 \tag{5}$$

where $\mathbf{L}$ is the operator

$$\frac{\partial^2}{\partial x^2} \tag{6}$$

Let us assume the solution to (5) is required over the domain $x = x_1$ to $x = x_2$, with the appropriate boundary condition applied at these points. Next the following integral (I) is employed

$$I = \int_{x_1}^{x_2} G_{(x)} \mathbf{L}c \, dx = \int_{x_1}^{x_2} G_{(x)} \frac{\partial^2 c}{\partial x^2} dx = \langle G, \mathbf{L}c \rangle \tag{7}$$

which is the product of the operator multiplied by an arbitary function $G(x)$. This inner product is usually reported in short hand notation as noted on the RHS of (7). Integration of eq 7 by parts (twice) gives the inverse formulation

$$I = \left[G\frac{dc}{dx}\right]_{x_1}^{x_2} - \left[\frac{dG}{dx}c\right]_{x_1}^{x_2} + \int_{x_1}^{x_2} c\frac{\partial^2 G}{\partial x^2} dx \tag{8}$$

where the x subscipt on G has been dropped for clarity. This approach results in an expression where the differential operator ($\mathbf{L}$) now acts on G not c. By convention the operator which acts on G is called adjoint and usually given the symbol $\mathbf{L}^*$. In this case $\mathbf{L}$ and $\mathbf{L}^*$ are the same (although this is not always the case). All of the additional terms of the RHS of eq 8 are values which are evaluated at the end points of the domain (x_1 and x_2). For clarity these boundary values are collected

together and represented by the symbol **B**. Therefore, in operator notation, (8) can be represented as

$$\langle G,\mathbf{L}c\rangle = \mathbf{B} + \langle c,\mathbf{L}^*G\rangle$$

G is defined as a weighting function which satisfies

$$\mathbf{L}^*c = 0 \tag{9}$$

or the product is equal to a Dirac delta (δ) function at the point $x = \xi$

$$\mathbf{L}^*c = -\delta(x - \xi) \tag{10}$$

under these specific conditions the differential operator is eliminated from the formulation. In the latter case the calculation proceeds via a fundamental solution method, in the former using a homogeneous solution.[21] We focus only on the application of the fundamental solution approach in this article. For one-dimensional problems G can be simply chosen as $x - x_1$ or $x_2 - x$, where x_1 and x_2 represent the boundaries of a region x. By using two weighting functions and substituting the boundary conditions into (8), it is possible to directly solve for the unknowns (concentration or flux) at the limits x_1 and x_2. The BE formulation of the two- and three-dimensional Laplace equation follows an almost identical route to the above. Although it is important to note that the solution of these formulations differs from the one-dimensional formulation, the details of which are now noted.

In the case of the two-dimensional analogue of (3) the integration procedure must now be performed in both the x and y planes, but otherwise is essentially identical to above.[21] The fundamental solution required is derived from

$$\frac{\partial^2 G}{\partial x^2} + \frac{\partial^2 G}{\partial y^2} = -\delta(x - 1\xi_1)(y - \xi_2) \tag{11}$$

where ξ_1 and ξ_2 represent the x and y coordinates in an analogus manner to (10). This results in the following expression for the 2D formulation:

$$-c_\mathrm{I} + \int_\Omega \left[G\frac{\partial c}{\partial n} - c\frac{\partial G}{\partial n}\right]\mathrm{d}\Omega = 0 \tag{12}$$

where c_i represents the concentration at the point (ξ_1,ξ_2). The boundary (Ω) is divided into a number of interconnecting elements (Ne) which have a constant flux or concentration, (Figure 2a), further details of which may be found in ref 22. The numerical procedure then involves moving the point (ξ_1,ξ_2) to each individual element and performing a numerical integration. Due to this procedure it simpler to express the fundamental solution in axisymmetric form to calculate the distance between the source point and the element under integration. Without any loss of generality for (11) this gives

$$G(x,y,\xi_1,\xi_2) = -\frac{1}{2\pi}\ln r$$

where r is the distance between the integration point and the source point

$$r = ((x - \xi_1)^2 + (y - \xi_2)^2)^{1/2}$$

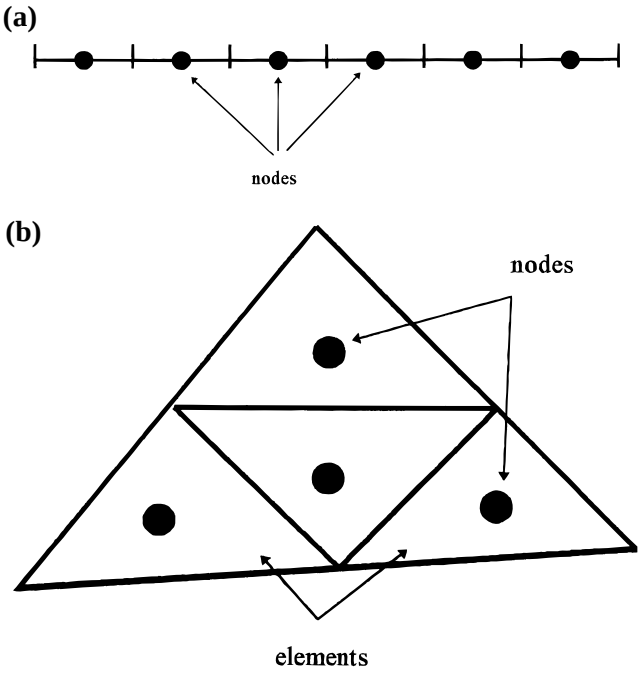

Figure 2. Schematic of the constant elements employed in the solution of (a) the two-dimensional and (b) the three-dimensional Laplace equation.

Formulation of the axismmetric form of (11) follows an identical path further deatils of whcih may be found in ref 22. This approach results in a coefficient matrix (Ne $\times$ Ne) in size with (Ne) unknowns (either concentration or flux). This problem can then be solved using standard matrix inversion routines.

For the three-dimensional form of (3) the integration procedure is performed over x, y, and z coordinates. The fundamental solution satisfies

$$\frac{\partial^2 G}{\partial x^2} + \frac{\partial^2 G}{\partial y^2} + \frac{\partial^2 G}{\partial z^2} = -\delta(x - \xi_1)(y - \xi_2)(z - \xi_3)$$

where ξ_1, ξ_2, and ξ_3 represent the coordinates of a concentrated heat source. This gives

$$G(x,y,z,\xi_1,\xi_2,\xi_3) = \frac{1}{4\pi r}$$

where r is again the distance between the integration point and the source point

$$r = ((x - \xi_1)^2 + (y - \xi_2)^2 + (z - \xi_3)^2)^{1/2}$$

The numerical procedure now requires the surface of the domain to be divided in to elements. We have employed triangular elements for this purpose all of which have either a fixed flux or concentration (Figure 2b). The solution of the system equations then follows an identical path to that of the two-dimensional problem, with the source point moved to each individual element to create a matrix which is then solved numerically for the unknowns.

All routines were written in Fortran 77 or 90 and run on a Pentium 166 PC, with 48 MB Ram. Run times varied between 5 s and 10 min depending upon the problem of interest.

Results and Discussion

First calculations were performed using the one-dimensional procedures. The diffusional flux was calculated along a line

TABLE 1: Diffusional Flux as a Function of Distance (x) Calculated Using the BE Method (s) and Analytically (t)

$\left(\frac{x}{D}\right)$	flux (s)	flux (t)
0.125	0.979	1.0
0.250	0.977	1.0
0.375	0.978	1.0
0.500	0.980	1.0
0.625	0.983	1.0
0.750	0.988	1.0
0.875	0.993	1.0
1.000	1.000	1.0

TABLE 2: Variation of Current Density as a Function of Electrode Radii for a Microdiscelectrode Predicted by BE Simulations and Analytically

$\left(\frac{R}{D}\right)$	$\left(\frac{I_{\text{simulation}}}{\text{F}}\right)$	$\left(\frac{I_{\text{analytical}}}{\text{F}}\right)$
1.0	4.008	4.00
2.0	8.025	8.00
3.0	12.04	12.0
4.0	16.07	16.0
5.0	20.09	20.0
6.0	24.11	24.0
7.0	28.13	28.0
8.0	32.15	32.0
9.0	36.18	36.0
10.0	40.18	40.0

with boundaries at x_1 and x_2, subject to the following conditions

$$x = x_1 \qquad c = 0$$

$$x = x_2 \qquad c = 1$$

The resulting diffusional flux at $x = x_1$ is noted in Table 1 as a function of the distance x, using a diffusion coefficient of 1×10^{-5} cm^2 s^{-1}. The normalized values calculated were in excellent agreement with those predicted analytically. A more detailed discussion of the one-dimensional simulations can be found in ref 23 where the simulations have been applied to steady state and transient: diffusion, diffusion-reaction and convection- diffusion-reaction problems.

Next simulations were performed using an axisymmetric BE formulation in 2 dimensions. A microdisk electrode of varying radius was examined initially for which an analytical solution has been reported previously.[24] Figure 3a shows a schematic of the grid employed for the simulations. The boundary conditions employed were such that a mass transport limited one electron reduction was induced on the microdisk electrode. The outer nonconducting sheaf was modeled using a no flux condition with the edge and top boundaries fixed at a normalized concentration of 1. Table 2 shows the variation of current as a function of normalized electrode radius simulated via the BE method using 200 elements. Also shown in Table 2 are the values predicted via analytical theory; in all simulations performed the error was found to be no more than 1% of the analytical current density.

Next a micohemispherical electrode was examined and a typical simulation grid is shown in Figure 3b. Switching between the disk and hemisphere geometries only requires a redifintion of element coordinates and thus is a simple procedure. The applied boundary conditions are identical to that for the microdisk electrode above. Table 3 shows the calculated and analytical values for this problem and again good agreement is observed. Having established the validity of our models we next examined how the current density varies as the curvature of the hemispherical electrode is progressively reduced toward the microdisk arrangement. Figure 3c shows a schematic of the geometries studied. The z direction radius (C/D) was scaled from a factor of 1 (corresponding to the hemisphere) to 0 (corresponding to the microdisk). Figure 4a shows how the normalized current (with respect to that of a microdisk electrode) varies as function of the factor z. Also shown is the analytical result predicted using results published previously.[25] Overall the current density is seen to go through a small maximum before dropping as the hemispherical geometry is reached. Examination of the current

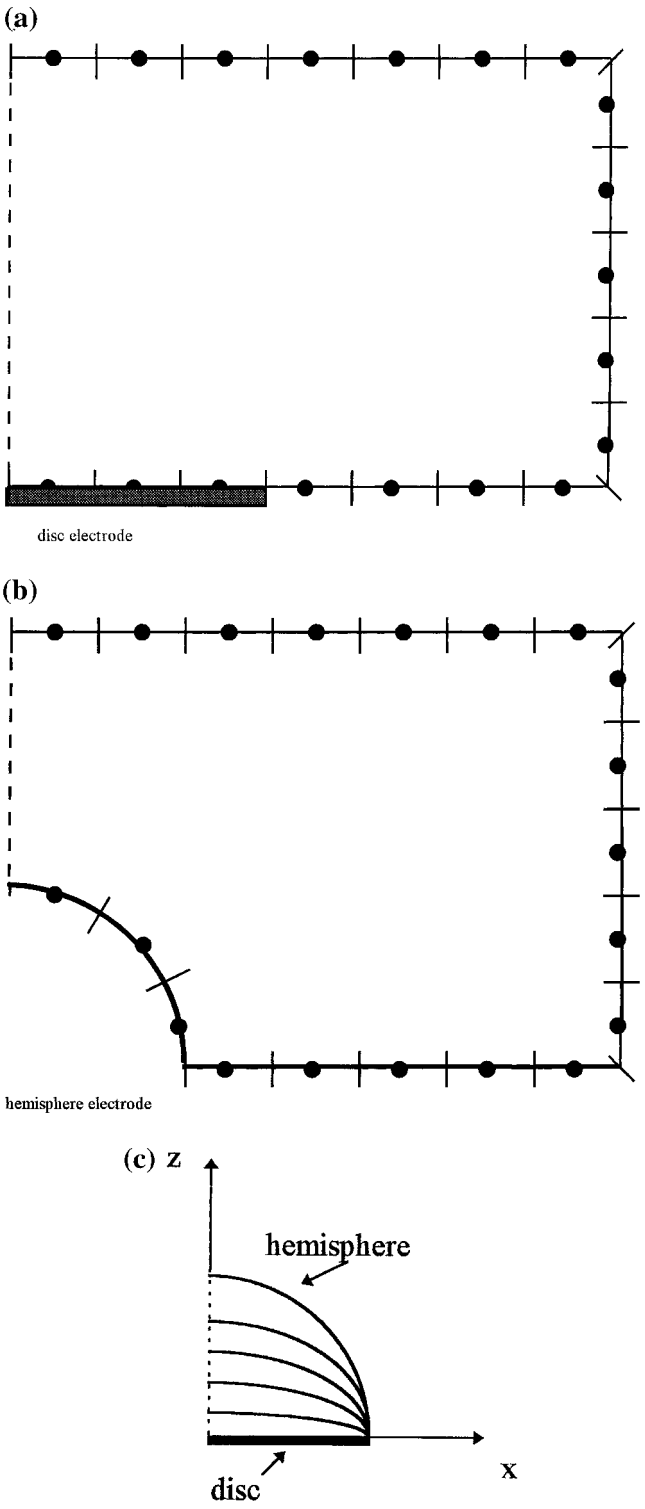

Figure 3. Schematic of the computational grids employed for the simulation of (a) a microdisk electrode, (b) a microhemispherical electrode, and (c) the transition between the two geometries.

TABLE 3: Variation of Current Density as a Function of Electrode Radii for a Microhemispherical Electrode Predicted by BE Simulations and Analytically

$\left(\frac{R}{D}\right)$	$\left(\frac{I_{\text{simulation}}}{\text{F}}\right)$	$\left(\frac{I_{\text{analytical}}}{\text{F}}\right)$
1	6.31	6.28
2	12.63	12.56
3	18.94	18.84
4	25.26	25.13
5	31.58	31.41
6	37.89	37.69
7	44.22	43.98
8	50.51	50.26
9	56.83	56.54
10	63.15	62.83

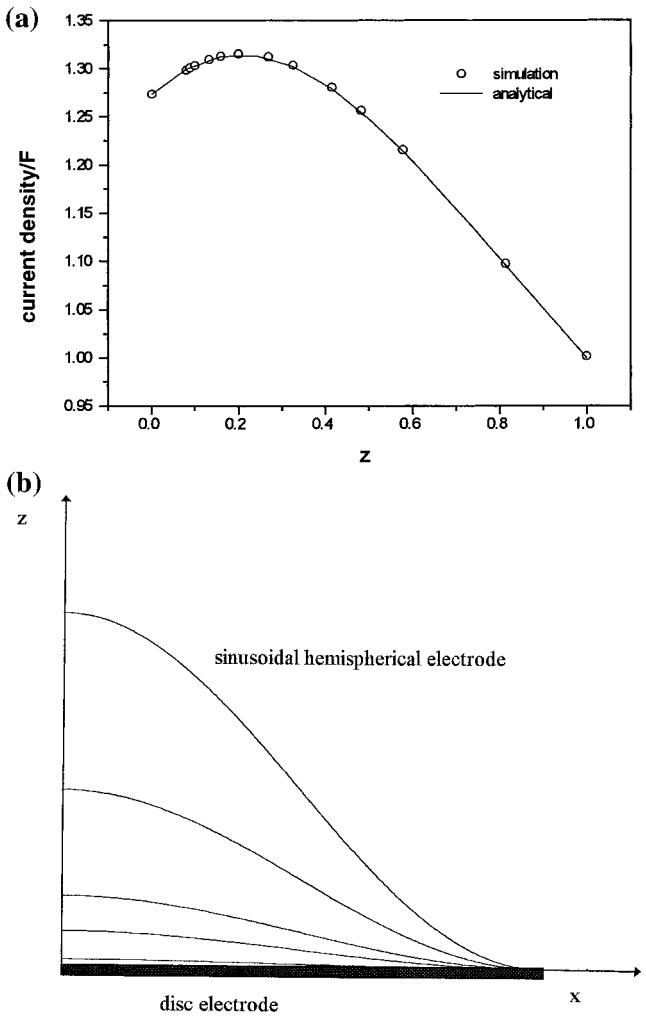

Figure 4. (a) Variation of current density predicted by BE simulations and analytically as a function of the curvature parameter *z*. (b) Schematic of the electrodes simulated using (13) as a function of parameter *z*.

density reveals a slight enhancement to the object center as the disk is intially distorted leading to a slightly higher current density. Greater distortion of the disk results in the edge effect becoming progressively less significant and the current density consequently approaches that expected for a hemispherical electrode. As an illustration of the flexibility of our strategy the axisymmetric simulations are finally employed to address a geometry which is analytically unexplored. We use the formula

$$y = A\left\{1 + \sin\left(\frac{\pi}{2} + \pi x\right)\right\} \qquad (13)$$

to generate a surface between $x = 0$ and $x = 1$ and $A = 0.005$ to $A = 0.5$. Figure 4b shows the resulting electrode geometries. Table 4 presents the results for these simulations along with the correponding value of A.

TABLE 4: Variation of Current Density as a Function of Electrode Radii for a Microelectrode Whose Surface Is Predicted Using Expression 13

A	area	current/F	current density/F
0.005	3.141 79	4.011 64	1.276 86
0.01	3.142 37	4.017 08	1.278 36
0.0125	3.142 8	4.019 62	1.278 99
0.01667	3.143 74	4.024 31	1.280 1
0.025	3.146 43	4.033 99	1.282 08
0.05	3.160 88	4.065 88	1.286 31
0.0625	3.171 65	4.083 16	1.287 39
0.08333	3.194 74	4.113 4	1.287 55
0.1	3.217 72	3.138 94	1.286 3
0.11111	3.235 19	4.157 28	1.285 02
0.125	3.259 4	4.180 6	1.282 63
0.14286	3.294 24	4.212 37	1.278 71
0.16667	3.346 92	4.257 27	1.272
0.2	3.431 78	4.324 97	1.260 27
0.22727	3.510 07	4.384 65	1.249 16
0.25	3.580 85	4.436 16	1.238 86
0.3125	3.798 37	4.589 6	1.208 31
0.35714	3.971 33	4.707 65	1.185 41
0.41667	4.220 57	4.873 5	1.154 7
0.5	4.598 18	5.118 57	1.113 7

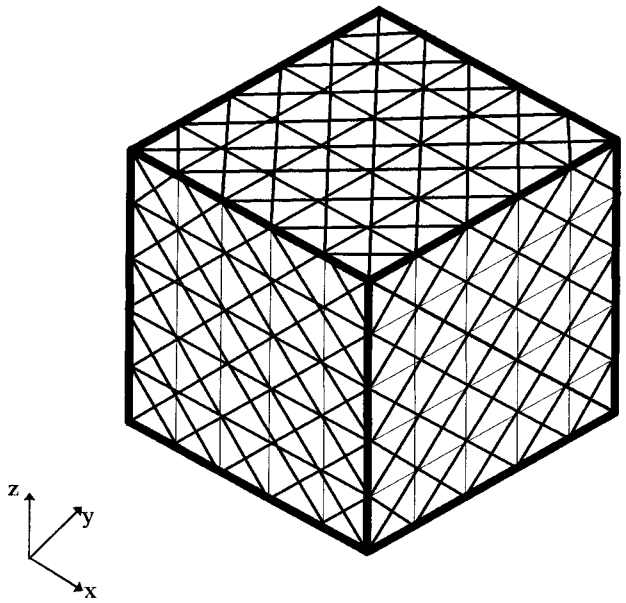

Figure 5. Schematic of three faces of the grid employed for three-dimensional steady-state simulations.

The above simulations show the versatility of our approach for modeling electrode geometries of an arbitary axisymmetric nature and offer the potential to map an electrode and simulate the response for the specific geometry. The final part of our work focused on a three-dimensional implementation of the BEM method with the potential to model true three-dimensional diffusion processes around "real" electrodes.

Three-dimensional simulations focused on the distortion of a microdisk electrode noted above. In this case we examined the current density as the edge curvature of an initial microdisk was altered. A three-dimensional grid was generated using triangular elements three faces of which are shown in Figure 5. For all simulations the electrode was sited on one face of the grid and noflux boundary condition applied to the region outside of the electrode. All other faces were set at a fixed normalized concentration of 1 as above. Preliminary simulations were

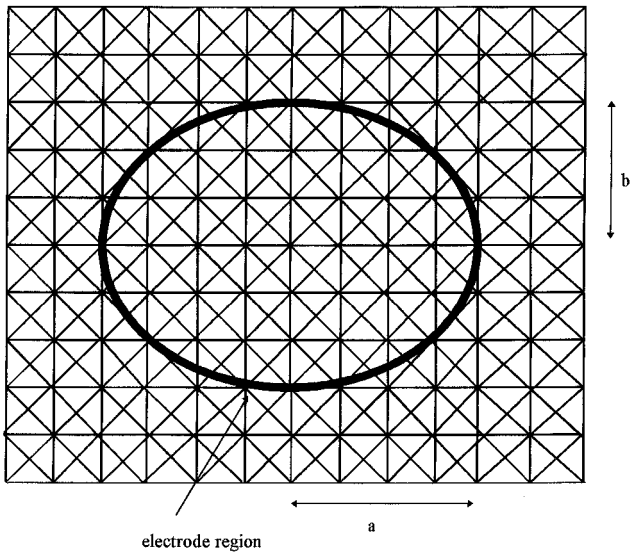

Figure 6. Illustration of the influence of the parameter *b* on the electrode geometry.

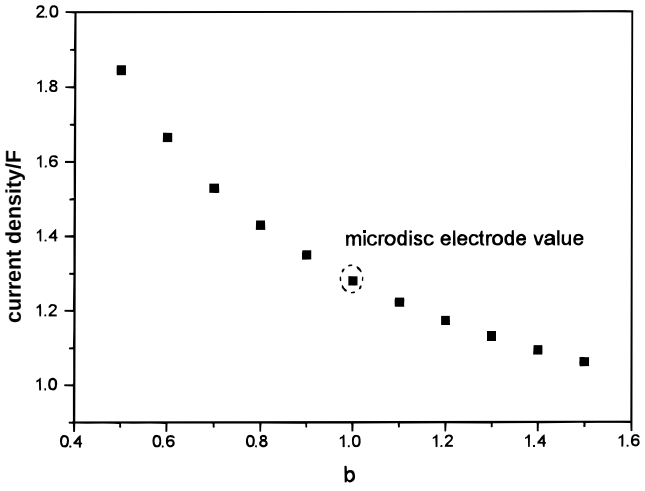

Figure 7. Variation of the current density as a function of the parameter *b*, for a microelectrode.

performed for a microdisk electrode as a test of our model. In all cases excellent agreement between the calculated current densities and those predicted analytically was observed. Next to illustrate the influence of edge curvature on the current density recorded the value of *b* was varied between 0.4 and 1.6 with $a = 1$. Figure 6 shows a schematic of one of the geometries and Figure 7 shows the variation of current density as a function of the length b. It is clear that as the disk is distorted to create sharpened points at the two extremes the current density rises, due to enhanced diffusion in the edge region. Corresponding a drop in edge effect is observed as the disk shape is approached. The magnitude of the effect can be seen to be relatively small even though the actual shape of the electrode has been distorted significantly. This result highlights to the experimentalist the potential difficulties of confirming from pure voltammetric measurements the regularity of microdisk electrodes.

Conclusion

The formulation and application of one, two and three-dimensional diffusion dominated electrochemical problems has been described. The BE method has been shown to offer an efficient and powerful tool for the simulation of electrodes of arbitary geometry. This approach provides the opportunity to map real electrode geometries using techniques such as AFM or STM and simulate the true three-dimensional current density of the system. The simulations can be routinely adapted to multiple electrode systems and therefore offers the opportunity to examine the effect of the overlap of diffusional fields from multiple sources.

Acknowledgment. We wish to thank the University of Bath for a University Studentship for support of Q.Fulian and the Nuffield Foundation for research support.

References and Notes

(1) Coyler, C. L.; Luscombe, D.; Oldham, K. B. *J. Electroanal. Chem.* **1990**, *283*, 379.
(2) Shultz, L. L.; Stoyanoff, J. S.; Nieman, T. A. *Anal. Chem.* **1996**, *68*, 349.
(3) Compton, R. G.; Unwin, P. R. *Comp. Chem. Kinet.* **1989**, *29*, 173.
(4) Fulian, Q.; Stevens, N. P. C.; Fisher, A. C. *J. Phys. Chem. B* **1998**, *102*. 3779.
(5) Bond, A. M. *Analyst* **1994**, *119*, 1.
(6) Feldberg, S. W. *Electroanal. Chem.* **1969**, *3*, 45.
(7) Britz, D. *Digital Simulation in Electrochemistry*; Sringer Verlag: Berlin, 1981.
(8) Shoup, D.; Szabo, A. *J. Electroanal. Chem.* **1984**, *160*, 17.
(9) Moldoveanu, J. L.; Anderson, J. *J. Electroanal. Chem.* **1984**, *179*, 107.
(10) Alden, J. A.; Compton R. G. *J. Electroanal. Chem.* **1996**, *404*, 27.
(11) Ziekiewicz, O. C. *The Finite Element Method in Engineering Science*, 2nd ed.; ed., McGraw-Hill: New York, 1977.
(12) Baker, A. J. *Finite element Computational Mechanics*, 1st ed.; McGraw-Hill: New York, 1983.
(13) Ramachandran, P. A. *Comput. Math.* **1990**, *19*, 63.
(14) Choi, Y. S.; Kang, T. *J. Electrochem. Soc.* **1996**, *143*, 480.
(15) Yan, J. F.; Pakalapati, S. N. R.; Nguyen T. V.; White R. E. *J. Electrochem. Soc.* **1992**, *139*, 1932.
(16) Ramachandran, P. A. *Chem. Eng. J.* **1990**, *45*, 49.
(17) Bossche, B. V. D.; Bortels, L.; Deconinck, J.; Vandeputte, S.; Hubin, A.; *J. Electroanal. Chem.* **1995**, *397*, 35.
(18) Bialecki, R.; Hahlik, R.; Lapkowski, M. *Electrochim. Acta* **1984**, *29*, 905.
(19) West, A. C.; Matlosz, M. *J. App. Electrochem.* **1994**, *24*, 261.
(20) Hume, E. C.; Deen, W. M.; Brown, R. A. *J. Electrochem. Soc.* **1984**, *131*, 1251.
(21) Ramachandran, P. A. *Boundary Element Methods in Transport Phenomena*, 1st ed.; Computational Mechanics Publications; Southampton and Elsevier, UK, 1994.
(22) Brebbia, C. A.; Dominguez, J. *Boundary Elements: An introductory course*, Computational Mechanics Publications; Southampton and McGraw-Hill: New York, 1989.
(23) Fulian, Q.; Fisher, A. C. *Electroanalysis* Submitted for publication.
(24) Fleischman, M.; Pons, S. *Ultramicroelectrodes*; Datatech: Morganton, NC, 1987.
(25) Roland Alfred, L. C.; Oldham K. B. *J. Phys. Chem.* **1996**, *100*, 2170.